Universal Phase Diagram for Wetting on Mesoscale Roughness

S. Herminghaus

Max-Planck-Institute for Dynamics and Self-Organization, Am Fassberg 17, 37077 Göttingen, Germany

(Received 28 August 2012; revised manuscript received 24 September 2012; published 5 December 2012)

The wetting properties of solid substrates with mesoscale (between van der Waals tails and the capillary length) random roughness are considered as a function of the microscopic contact angle of the wetting liquid and its partial pressure in the surrounding gas phase. It is shown that the well-known transition occurring at Wenzel's angle is accompanied by a transition line at which a jump in the adsorbed liquid volume occurs. This should be present generally on surfaces bearing homogeneous, isotropic random roughness. While a similar abrupt filling transition has been reported before for certain idealized groove or trough geometries, it is identified here as a universal phenomenon. Its location can be analytically calculated under certain mild conditions.

DOI: 10.1103/PhysRevLett.109.236102 PACS numbers: 68.05.−n, 05.40.−a, 64.75.−g, 68.08.−p

The physics of wetting and spreading on ideally smooth surfaces has meanwhile reached the status of mature textbook knowledge [1–4]. In contrast, the wetting properties of randomly rough solid substrates, which are by far more relevant, are still poorly understood. This is in part due to the wide range of scales to be covered, which extends from the submicron scale to the scale of millimeters, just before gravity comes into play. Aside from treatments on the nanometer scale [5–9], which is not dominant for most roughnesses encountered on real surfaces, most authors have tried to model rough surfaces as Gaussian random processes [10–17], or to capture single aspects of wetting using simplified model geometries [18–26]. For the latter approach, it has been shown that for variable contact angle and vapor pressure, some of the idealized geometries exhibit a filling transition, and some do not [20,21]. In this Letter, it is shown that the filling transition is indeed the generic case for a wide range of roughnesses occurring naturally. A method for analytically calculating the corresponding phase diagram is given.

Wenzel was the first to provide a systematic study of wetting on mesoscopically rough surfaces [27]. By mesoscopic we mean, on the one hand, larger than the typical ranges of wetting forces (such as van der Waals, of order several nanometers), such that a microscopic contact angle is well defined (furthermore, line tension effects can be safely neglected on that scale [28–30]). On the other hand, we consider only roughness that is small as compared to the capillary length of the liquid, such that gravity effects can as well be neglected. Note that most roughness encountered customarily falls in that "mesoscopic" range. Wenzel characterized the roughness by a single parameter, r, which he defined as the ratio of the total substrate area divided by its projected area. Obviously, $r \geq 1$, and $r = 1$ corresponds to a perfectly smooth surface. The free energy which is gained when the rough substrate is covered with a liquid is then given by $r(\gamma_{sg} - \gamma_{sl})$, where γ_{sl} and γ_{sg} are the solid-liquid and solid-gas interfacial tension, respectively. If this gain is larger than the surface tension of the liquid, γ, we expect a vanishing *macroscopic* contact angle, because covering the substrate with the liquid releases more energy than is required for the formation of a free liquid surface of the same (projected) area. More specifically, force balance at the three-phase contact line yields

$$\cos\theta_{\mathrm{macro}} = \frac{r(\gamma_{sg} - \gamma_{sl})}{\gamma} = r\cos\theta \tag{1}$$

where $\theta = \arccos[(\gamma_{sg} - \gamma_{sl})/\gamma]$ is the microscopic contact angle [31]. When θ is reduced to $\theta_W = \arccos(1/r)$, θ_{macro} vanishes, and the substrate is covered with an "infinitely" thick liquid film. In the present Letter, we explore the vicinity of this transition in some detail, both at liquid-vapor coexistence and below the saturated vapor pressure.

We describe the rough solid substrate by a function $f(x, y)$, which shall approximate the actual physical surface at any required precision, but be mathematically smooth, such that ∇f and Δf exist everywhere. The roughness is assumed to be homogeneous and isotropic; i.e., its statistical parameters shall be the same everywhere on the sample, and independent of rotation of the sample about its normal axis. A small amount of liquid deposited on this substrate will make an interface with the surrounding gas, which is described by a second function, $g(x, y)$. The support of g is the wetted area, which we call $\mathcal{W}$. Continuity of the liquid surface assures $g = f$ on the boundary of $\mathcal{W}$, i.e., the projection of the three-phase contact line, henceforth denoted by $\partial\mathcal{W}$ [cf. Fig. 1(a)].

As the amplitude of most natural roughness is much smaller than its dominant lateral length scale, we assume that

$$|\nabla f| \ll 1 \tag{2}$$

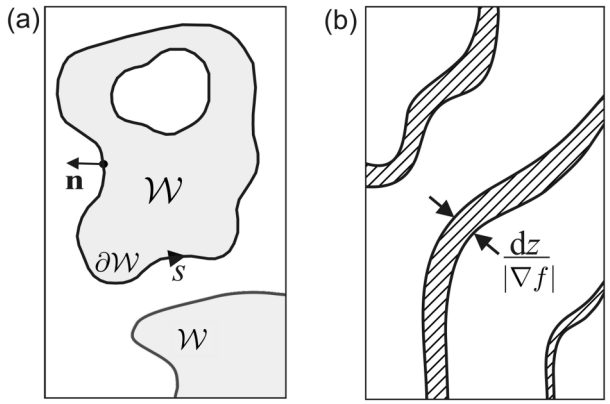

FIG. 1. (a) Top view of the sample, showing the wetted areas in grey, the bare substrate in white. The normal vector to $\partial\mathcal{W}$, $\mathbf{n}$, lies in the (x, y) plane. (b) Two sets of contour lines of f at heights z and $z + dz$. The hatched area between the lines is equal to $p(z)dz$.

which allows for substantial simplifications. The same shall hold for g. The contact angle with the substrate, θ, yields the boundary condition

$$|\nabla(g - f)| \approx \tan\theta \approx \theta \tag{3}$$

which is to be fulfilled everywhere on $\partial\mathcal{W}$, to first order in θ, ∇f, and ∇g. This determines the morphology of the liquid-vapor interface, and thereby $\partial\mathcal{W}$ and the amount of adsorbed liquid. Applying Green's theorem to $(g\text{-}f)$, we obtain

$$\int_{\partial\mathcal{W}} \mathbf{n}\cdot\nabla(g - f)ds = \int_{\mathcal{W}} \Delta(g - f)d^2\mathbf{x} \tag{4}$$

where s is the distance along $\partial\mathcal{W}$, $\mathbf{n}$ its unit normal vector, and $\mathbf{x} = (x, y)$. Since $g = f$ on $\partial\mathcal{W}$, $\nabla(g - f)$ is perpendicular to $\partial\mathcal{W}$ everywhere. Hence Eq. (3) may be written as $\mathbf{n}\cdot\nabla(g - f) \approx \theta$, and Eq. (4) can be recast into

$$l\theta + \int_{\mathcal{W}} [2H - \Delta f]d^2\mathbf{x} = 0 \tag{5}$$

in which l denotes the length of $\partial\mathcal{W}$, and $H \approx \frac{1}{2}\Delta g$ is the mean curvature of the liquid-vapor interface. The latter is given by the Kelvin equation,

$$H = \frac{k_B T}{2\gamma v_m} \ln\frac{\mathrm{p}_s}{\mathrm{p}} \tag{6}$$

where p is the partial pressure of the adsorbed liquid in the surrounding gas phase, p_s is its saturated vapor pressure, v_m its molecular volume, and k_B is Boltzmann's constant. It is a convenient measure for the deviation from liquid-vapor coexistence.

Before we can exploit Eq. (5), we derive a few useful relations. If $p(f)$ is the height distribution of $f(\mathbf{x})$, the total area between the contour lines at $f = z$ and at $f = z + dz$ is given by $p(z)dz$, which corresponds to the hatched area in Fig. 1(b). The average slope on that set, $\sigma_1(z) = \langle|\nabla f|\rangle_z$, is given by

$$\sigma_1(z) = \frac{\int |\nabla f(z)|d\tau}{p(z)dz} \tag{7}$$

where $d\tau = dsdz/|\nabla f(z)|$ is the differential of the hatched area. Hence for the total length of the contour line at height z we obtain

$$L(z) = \int ds = \sigma_1(z)p(z). \tag{8}$$

Next we apply Green's theorem to Δf, this time to the area enclosed by the contour line at $f = z$. This yields

$$\int_{\mathcal{C}(z)} \Delta f d^2\mathbf{x} = \int_{\partial\mathcal{C}} \mathbf{n}\cdot\nabla f ds \tag{9}$$

where $\mathcal{C}(z)$ is the set $\{\mathbf{x} \mid f(\mathbf{x}) \le z\}$, and $\partial\mathcal{C}$ its boundary, i.e., the contour line itself. Introducing $\sigma_2(z) = \langle|\nabla f|^2\rangle_z$, we readily see that Eq. (9) can be rewritten as

$$\int_{\mathcal{C}(z)} \Delta f d^2\mathbf{x} = \sigma_2(z)p(z). \tag{10}$$

The vertical position of the three-phase contact line, which may be symbolically written as $f(\partial\mathcal{W})$, will vary along $\partial\mathcal{W}$ about an average value, $h = \langle f(\partial\mathcal{W})\rangle$. The projection of the contact line onto the plane will thus approximately follow the contour line at $f(\mathbf{x}) = h$, with excursions towards both the outside and the inside of $\mathcal{W}$. These will in cases represent detours, sometimes shortcuts with respect to $\partial\mathcal{W}$. As a reasonable approximation, we may thus use $l \approx L(h)$ for the length of the three-phase contact line. Similarly, we set

$$\int_{\mathcal{W}} d^2\mathbf{x} \approx \int_{-\infty}^{h} p(z)dz = W(h) \tag{11}$$

for the wetted sample area. Inserting these expressions in Eq. (5), we obtain

$$2HW(h) \approx \left[\frac{\sigma_2(h)}{\sigma_1(h)} - \theta\right]L(h). \tag{12}$$

This allows, if $p(h)$, $\sigma_1(h)$, and $\sigma_2(h)$ are known from experimental characterization of the sample, to determine the adsorbed amount of liquid, V, as a function of θ and H. V is related to h via

$$V = \int_{h_-}^{h} (h - f)p(f)df, \tag{13}$$

and can be evaluated if h and $p(f)$ are known. However, we continue here to discuss h instead, since it is more accessible through the formalism developed above.

Up to this point, we have not made any specific assumption about the roughness profile, except it being sufficiently shallow for the approximations made above to hold. Now we shall go one step further, observing that roughness profiles generated by wear, weathering, erosion, etching,

sand blasting, or similar processes will invariably have a finite codomain (we disregard fissures and cracks here). In other words, the support of $p(z)$ is the interval $[z_-, z_+]\forall \mathbf{x}$, where z_- represents the depth of the deepest trough, and z_+ the height of the highest elevation on the sample. This has severe consequences for σ_1 and σ_2, as both must go to zero as $z \to z_\pm$. To see that, consider the distribution of minima, $\mu_-(z)$. Clearly, $\mu_- \to 0$ for $z \to z_-$, and we may choose to write $\mu_-(z) \simeq \mu_0(z - z_-)^\nu$, with some $\nu > 0$. Since each minimum is parabolic to first order, one can readily verify that it contributes $4\pi(z - z_0)$ to σ_1, if z_0 is the depth of the minimum. We thus have

$$\sigma_1(h) \leq 4\pi \int_{z_-}^{h} \mu_-(z)(h - z)dz \simeq \frac{\mu_0(h - z_-)^{\nu+2}}{(\nu + 1)(\nu + 2)}. \tag{14}$$

The "$\leq$" sign has been used because there may be saddle points (or even maxima) occurring at elevations between h_- and h, which can only reduce σ_1. As Eq. (14) shows, $\sigma_1(h)$ is bounded from above by a function which vanishes at least quadratically as $h \to z_-$. An analogous result is obtained for $h \to z_+$.

Next we consider the ratio σ_1/σ_2. With the abbreviation $\rho = |\nabla f|$, we have

$$\sigma_1(h) = 2\pi \int \rho^2 q(h, \rho)d\rho \tag{15}$$

where $q(h, \rho)$ is the distribution of slopes, sampled at height h. Similarly, we have

$$\sigma_2(h) = 2\pi \int \rho^3 q(h, \rho)d\rho. \tag{16}$$

As a consequence,

$$\frac{\sigma_2(h)}{\sigma_1(h)} = \frac{\int \rho^3 q(h, \rho)d\rho}{\int \rho^2 q(h, \rho)d\rho} < \rho_{\max}(h) \tag{17}$$

where $\rho_{\max}$ is the maximum slope encountered at elevation h. Since this vanishes as $h \to z_-$ as σ_1 does, so will the ratio σ_2/σ_1, as Eq. (17) shows.

Aside from these global properties, both σ_1 and σ_2 are expected to be largely featureless, due to the general fact that the processes leading to roughness exhibit only very limited lateral correlation. For any pronounced feature to develop in σ_i, distant places on the sample would have to "conspire" to contribute to that feature at the same depth. This can happen only for composite surfaces, where the roughness topography may penetrate through a coating or other stratigraphic variation of material properties. Such ramifications are interesting to consider for practical purposes, but well beyond the scope of the present article.

The generic shape of the function

$$\Lambda(h) = \left[\frac{\sigma_2(h)}{\sigma_1(h)} - \theta\right] \tag{18}$$

which appears in Eq. (12) is sketched in Fig. 2, according to the discussion above. Following Eq. (12), the film thickness at coexistence ($H = 0$) can be derived from the zeros of Λ, of which there are either two or none, depending on θ. In the latter case, the contact angle is too large for forming a liquid surface between the spikes and troughs which complies with the boundary condition, Eq. (3). If, however, $\Lambda(h)$ intersects the h axis, the slopes of the zeros decide upon the stability of the corresponding solutions. This can be seen by appreciating that Λ may be interpreted as a deviation from the force balance expressed by Eq. (3). For the left zero, which is marked by an open circle in the figure, a displacement of the three-phase contact line would give rise to an imbalance of wetting forces which drives it further away from the zero. The opposite is true for the right zero, marked by the closed circle. The latter therefore corresponds to the stable solution, and thus to the adsorbed film thickness which will develop. All this is in marked contrast to Gaussian roughness, which has been frequently invoked for reasons of mathematical tractability, but strictly speaking does not occur in nature. For Gaussian roughness, σ_1 and σ_2 are independent of h, with $\sigma_2/\sigma_1 = 4/\pi \forall h$ [32]. This is in fact a dramatic difference, as Λ would then just be a horizontal straight line which lies either above or below the h axis depending on θ. As a consequence, the whole structure we are developing here would be absent.

The graph of $\Lambda(h)$ makes contact with the horizontal axis when θ reaches

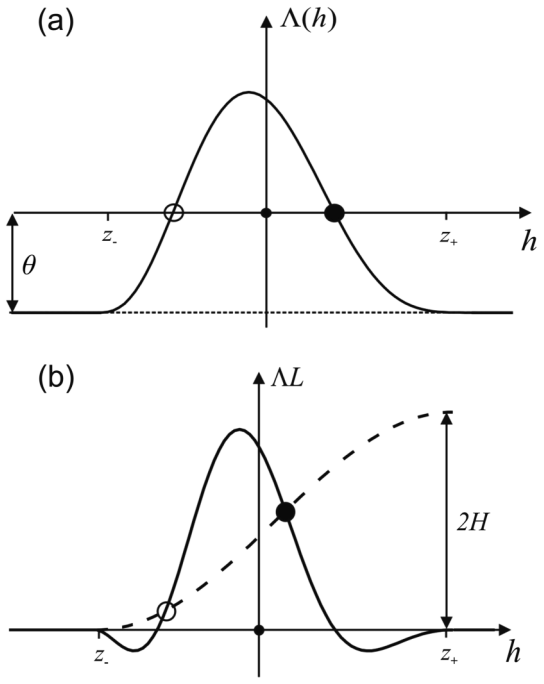

FIG. 2. Graphic construction for solving Eq. (12). The dashed line represents the left-hand side of Eq. (12).

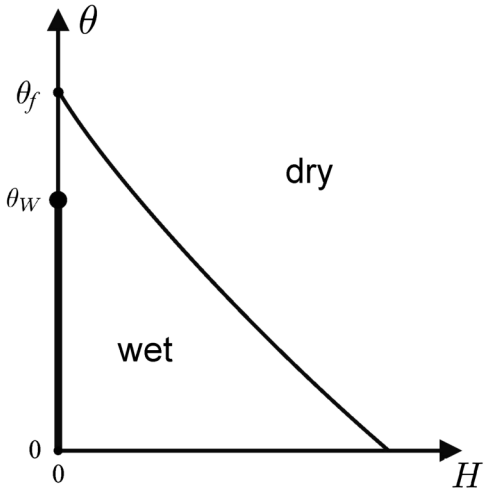

FIG. 3. The phase diagram for wetting on surfaces with homogeneous, isotropic roughness. The most prominent feature is the existence of a transition line $[H_f(\theta)]$, at which the adsorbed average film thickness [and thereby the liquid coverage, Eq. (13)] jumps discontinuously from zero to a finite value.

$$\theta_f = \max\left(\frac{\sigma_2}{\sigma_1}\right). \tag{19}$$

At this point, the formerly dry substrate is covered with a liquid film of "thickness" $h_f = \mathrm{argmax}(\sigma_2/\sigma_1)$. It is important to note that θ_f always lies above θ_W. To see this, we note that $r = 1/\cos\theta_W \approx 1 + \frac{1}{2}\theta_W^2$. Furthermore, $r = \langle\sqrt{1 + |\nabla f|^2}\rangle$. Thus we have

$$\theta_W^2 \approx \frac{1}{|S|}\int_{h_-}^{h_+} \sigma_2(h)p(h)dh < \max(\sigma_2). \tag{20}$$

On the other hand, $\sigma_2 > \sigma_1^2$, such that

$$\theta_f^2 = \max\left(\frac{\sigma_2}{\sigma_1}\right)^2 > \max(\sigma_2). \tag{21}$$

From Eqs. (20) and (21), it follows directly that $\theta_f > \theta_W$.

Let us now consider the system off coexistence, again invoking Eq. (12) as the condition determining h. A graphical solution of Eq. (12) is sketched in Fig. 2(b). As long as $\theta > 0$, both relevant zeros of $\Lambda L(h)$ [representing the solutions of Eq. (12) for $H = 0$] lie well within the interval $[z_-, z_+]$. For $H > 0$ (dashed curve), the closed circle indicates again the stable solution. Obviously, the two points of intersection will merge when the dashed and solid curves touch each other only at a single point. This occurs at a certain curvature $H_f(\theta)$ of the liquid surface. For $H > H_f$, solid and dashed curve meet only for $h \to z_-$: there is no liquid adsorbed, and the substrate is dry. Hence the average position of the liquid surface, h, and thus the surface coverage, jumps discontinuously at $H = H_f$. It is clear from the construction that H_f decreases monotonically with θ. As H is reduced below H_f, h increases continuously until at coexistence it reaches a value corresponding to the right zero of ΛL. When the microscopic contact angle is varied, a line of transitions results, which is shown in Fig. 3 as the solid curve.

We should not close without mentioning that the presence of roughness gives rise to substantial equilibration times, as saddle points and extrema occurring at elevations $h_0 \in [z_-, z_+]$ provide effective pinning centers [1,33,34]. However, transport through either the gas phase or through the molecular adsorbed film [35,36] will always allow equilibration over manageable times, since the lateral distances involved are never larger than the lateral length scale of the roughness.

In conclusion, it turns out that on customary rough surfaces, with homogeneous and isotropic random roughness on length scales large as compared to molecular scales (but smaller than the capillary length) should quite generally exhibit a filling transition at contact angles larger than those where the Wenzel transition occurs. This filling transition is accompanied by a line of transitions reaching away from liquid vapor coexistence.

This finding may be of importance, e.g., for transport processes in soils, since typical roughness length scales encountered on many hard solid surfaces, like on grains of minerals, entail a filling transition at liquid surface curvatures encountered a few centimeters up to few meters above the water table. It is therefore conceivable that the liquid transport processes in the vadose zone are strongly influenced by the wetting phase diagram proposed above.

Inspiring discussions with Daniel Tartakovsky, Siegfried Dietrich, Tom Witten, Martin Brinkmann, Jürgen Vollmer, Sabine Klapp, and Daniela Fliegner are gratefully acknowledged. The author furthermore acknowledges generous support form BP International Inc. within the ExploRe research program.

[1] P. G. de Gennes, Rev. Mod. Phys. **57**, 827 (1985).
[2] S. Dietrich, in *Phase Transitions and Critical Phenomena*, edited by C. Domb and J. L. Lebowitz (Academic Press, London, 1988), Vol. 12.
[3] P.-G. de Gennes, F. Brochard-Wyart, and D. Quéré, *Capillarity and Wetting Phenomena: Drops, Bubbles, Pearls, Waves* (Springer, New York, 2004).
[4] D. Bonn, J. Eggers, J. Indekeu, J. Meunier, and E. Rolley, Rev. Mod. Phys. **81**, 739 (2009).
[5] K. M. Jansons, J. Fluid Mech. **154**, 1 (1985).
[6] D. Andelman, J.-F. Joanny, and M. O. Robbins, Europhys. Lett. **7**, 731 (1988).
[7] R. R. Netz and D. Andelman, Phys. Rev. E **55**, 687 (1997).
[8] P. S. Swain and R. Lipowsky, Langmuir **14**, 6772 (1998).
[9] T. S. Chow, J. Phys. Condens. Matter **10**, L445 (1998).
[10] P. R. Nayak, Wear **26**, 305 (1973).
[11] J. A. Greenwood, Proceedings of the Royal Society of Canada Deliberations de la Societe royale du Canada **393**, 133 (1984).

[12] P. Pfeifer, Y. J. Wu, M. W. Cole, and J. Krim, Phys. Rev. Lett. **62**, 1997 (1989).
[13] G. Palasantzas and J. Krim, Phys. Rev. B **48**, 2873 (1993).
[14] J. A. Ogilvy and J. R. Foster, J. Phys. D **22**, 1243 (1989).
[15] M. Kardar and J. O. Indekeu, Europhys. Lett. **12**, 161 (1990).
[16] N. Savva, S. Kalliadasis, and G. A. Pavliotis, Phys. Rev. Lett. **104**, 084501 (2010).
[17] M. A. Rodriguez-Valverde, P. J. Ramon-Torregosa, and M. A. Cabrerizo-Vilchez, in *Microscopy: Science, Technology, Application and Education*, edited by A. Mendez-Vilaz and J. Diaz, Estimation of Percolation Threshold of Acid-etched Titanium Surfaces using Minkowski Functionals Vol. 3 (Formatex Research Center, Spain, 2010), pp. 1978–1983.
[18] E. Cheng and M. W. Cole, Phys. Rev. B **41**, 9650 (1990).
[19] M. Napiorkowski and S. Dietrich, Phys. Rev. E **47**, 1836 (1993).
[20] C. Rascon and A. Parry, Nature (London) **407**, 986 (2000).
[21] A Sartori and A. Parry, J. Phys. Condens. Matter **14**, L679 (2002).
[22] R. Seemann, M. Brinkmann, E. J. Kramer, F. F. Lange, and R. Lipowsky, Proc. Natl. Acad. Sci. U.S.A. **102**, 1848 (2005).
[23] S. Herminghaus, M. Brinkmann, and R. Seemann, Annu. Rev. Mater. Res. **38**, 101 (2008).
[24] J. Courbin, J. C. Bird, M. Reyssat, and H. A. Stone, J. Phys. Condens. Matter **21**, 464127 (2009).
[25] J. Bico, C. Tordeux, and D. Quéré, Europhys. Lett. **55**, 214 (2001).
[26] J. Bico, U. Thiele, and D. Quéré, Colloids Surf. A **206**, 41 (2002).
[27] R. N. Wenzel, Ind. Eng. Chem. **28**, 988 (1936).
[28] T. Pompe and S. Herminghaus, Phys. Rev. Lett. **85**, 1930 (2000).
[29] P. G. Cao, K. Xu, J. O. Varghese, and J. R. Heath, Nano Lett. **11**, 5581 (2011).
[30] J. H. Weijs, A. Marchand, B. Andreotti, D. Lohse, and J. H. Snoeijer, Phys. Fluids **23**, 022001 (2011).
[31] T. Young, Phil. Trans. R. Soc. London **95**, 65 (1805).
[32] S. Herminghaus, Eur. Phys. J. E **35**, 43 (2012).
[33] J. F. Joanny and P. G. DeGennes, J. Chem. Phys. **81**, 552 (1984).
[34] M. B. Isichenko, Rev. Mod. Phys. **64**, 961 (1992).
[35] R. Seemann, W. Mönch, and S. Herminghaus, Europhys. Lett. **55**, 698 (2001).
[36] T. Ala-Nissila, T. Hjelt, S. Herminghaus, and P. Leiderer, Phys. Rev. Lett. **76**, 4003 (1996).